Sampling-Aware Control Barrier Functions for Safety-Critical and Finite-Time Constrained Control

Shuo Liu¹, Wei Xiao² and Calin A. Belta³

Abstract—In safety-critical control systems, ensuring both safety and feasibility under sampled-data implementations is crucial for practical deployment. Existing Control Barrier Function (CBF) frameworks, such as High-Order CBFs (HOCBFs), effectively guarantee safety in continuous time but may become unsafe when executed under zero-order-hold (ZOH) controllers due to inter-sampling effects. Moreover, they do not explicitly handle finite-time reach-and-remain requirements or multiple simultaneous constraints, which often lead to conflicts between safety and reach-and-remain objectives, resulting in feasibility issues during control synthesis. This paper introduces Sampling-Aware Control Barrier Functions (SACBFs), a unified framework that accounts for sampling effects and high relativedegree constraints by estimating and incorporating Taylor-based upper bounds on barrier evolution between sampling instants. The proposed method guarantees continuous-time forward invariance of safety and finite-time reach-and-remain sets under ZOH control. To further improve feasibility, a relaxed variant (r-SACBF) introduces slack variables for handling multiple constraints realized through time-varying CBFs. Simulation studies on a unicycle robot demonstrate that SACBFs achieve safe and feasible performance in scenarios where traditional HOCBF methods fail.

I. INTRODUCTION

Safety is a fundamental consideration in the design and operation of autonomous systems. To ensure safety, extensive research has focused on incorporating safety constraints into optimal control formulations through the use of Barrier Functions (BFs) and Control Barrier Functions (CBFs). Originally introduced in the context of optimization [1], BFs are Lyapunov-like functions [2] that have been widely employed to establish set invariance [3], [4] and to develop multi-objective and multi-agent control strategies [5], [6].

CBFs generalize BFs to guarantee the forward invariance of safe sets for affine control systems. When a CBF satisfies Lyapunov-like conditions, system safety is ensured [7]. By integrating CBFs with Control Lyapunov Functions (CLFs), the CBF-CLF-QP framework formulates safe and optimal control problems as a sequence of Quadratic Programs (QPs) [7], [8]. Although early formulations were limited to constraints with relative degree one, subsequent extensions such as Exponential CBFs [9] and High-Order CBFs (HOCBFs) [10] have enabled handling of higher-order constraints. The

This work was supported in part by the NSF under grant IIS-2024606 at Boston University.

CBF-CLF-QP framework has been applied across various domains, including rehabilitation robotics [11], adaptive cruise control [12], [13], humanoid locomotion [14], and obstacle avoidance in complex environments [15], [16].

Recent works also employed CBFs or CLFs to enforce time-constrained or task-based specifications on the system trajectories, like [17]–[20]. In practice, physical systems evolve in continuous time, while controllers are typically implemented in discrete time, such as zero-order-hold (ZOH) controllers with a fixed sampling period. However, counterexamples can be readily constructed to show that control laws derived from the CBF conditions in [5], [21] may lose their safety guarantees when implemented in discrete time. Conversely, controllers designed using discrete-time CBFs may not guarantee continuous-time safety between sampling instants [22].

Recently, [23] proposed a method for ensuring satisfaction of the continuous-time CBF condition under a ZOH control law by bounding the time derivative of the CBF between sampling instants. [24] developed a self-triggered control framework for safety-critical systems that adaptively determines the next sampling time based on the CBF evolution, thereby reducing conservatism compared to fixed-period sampling. Subsequently, [25] presented a sampled-data formulation that guarantees forward invariance under ZOH implementation by explicitly accounting for inter-sampling effects. [26] proposed an approach that employs approximate discrete-time models to verify safety between sampling intervals. More recently, [27] incorporated both sampling and quantization effects into the CBF design to enhance the safety of cyber-physical systems implemented in digital environments. Despite these advances, existing approaches still have notable limitations. They primarily address constraints with relative degree one and thus cannot be directly extended to high-order constraints; they do not consider temporal constraints, which are usually realized through time-varying CBFs; and when multiple safety constraints are simultaneously imposed, the resulting optimization problems often suffer from infeasibility.

In this paper, we consider finite-time reach-and-remain requirements, which aim to guarantee that the system states reach a specified target set within a user-defined time horizon and subsequently remain within this set for a prescribed duration. Such requirements naturally arise when decomposing Signal Temporal Logic (STL) specifications into basic control objectives—primarily safety, reachability, and persistence constraints [17], [18]. To ensure safety and finite-time reachand-remain for nonlinear systems with high relative-degree constraints under ZOH control, we propose Sampling-Aware

¹S. Liu is with the department of Mechanical Engineering, Boston University, Brookline, MA, USA. liushuo@bu.edu

²W. Xiao is with Department of Robotics Engineering, Worcester Polytechnic Institute, MA, USA. wxiao3@wpi.edu

³C. Belta is with the Department of Electrical and Computer Engineering and the Department of Computer Science, University of Maryland, College Park, MD, USA calin@umd.edu

Control Barrier Functions (SACBFs). Specifically, we develop a unified framework of SACBFs that explicitly account for sampling effects and high relative-degree constraints. By incorporating Taylor-based estimates of the upper bounds on the barrier function evolution between sampling instants, the proposed SACBFs ensure continuous-time forward invariance of the sets for safety and finite-time reach-and-remain under ZOH control. To enhance feasibility when multiple constraints are simultaneously enforced, a relaxation variable is introduced to each constraint without compromising forward invariance. Furthermore, we define two candidate SACBF formulations to handle aforementioned requirements: one designed for safety with time-invariant structure, and the other for finite-time reach-and-remain realized through time-varying CBFs. The effectiveness and flexibility of the proposed framework are demonstrated through case studies on a unicycle robot, showing that the relaxed SACBF achieves safe and feasible performance where traditional HOCBF methods fail.

II. PRELIMINARIES

Consider an affine control system expressed as

$$\dot{\boldsymbol{x}} = f(\boldsymbol{x}) + g(\boldsymbol{x})\boldsymbol{u},\tag{1}$$

where $x \in \mathbb{R}^n$, $f : \mathbb{R}^n \to \mathbb{R}^n$ and $g : \mathbb{R}^n \to \mathbb{R}^{n \times q}$ are locally Lipschitz. The control is $u \in \mathcal{U} \subset \mathbb{R}^q$, where the control constraint set \mathcal{U} is defined as

$$\mathcal{U} \coloneqq \{ \boldsymbol{u} \in \mathbb{R}^q : \boldsymbol{u}_{min} \le \boldsymbol{u} \le \boldsymbol{u}_{max} \}, \tag{2}$$

with $u_{min}, u_{max} \in \mathbb{R}^q$ (vector inequalities are interpreted componentwise).

Definition 1 (Lipschitz continuity [28]). A function $h: \mathbb{R}^n \to \mathbb{R}^m$ is said to be Lipschitz continuous on a set $\mathcal{D} \subseteq \mathbb{R}^n$ if there exists a constant $L \geq 0$ such that

$$||h(\mathbf{x}) - h(\mathbf{y})|| \le L||\mathbf{x} - \mathbf{y}||, \quad \forall \mathbf{x}, \mathbf{y} \in \mathcal{D}.$$
 (3)

The smallest such L is called the Lipschitz constant of h.

Definition 2 (Class κ function [29]). A continuous function $\alpha:[0,a)\to[0,+\infty], a>0$ is called a class κ function if it is strictly increasing and $\alpha(0)=0$.

Definition 3. A set $C \subset \mathbb{R}^n$ is forward invariant for system (1) if its solutions for some $u \in \mathcal{U}$ starting from any $x(0) \in C$ satisfy $x(t) \in C, \forall t \geq 0$.

Definition 4. The relative degree of a differentiable function $b: \mathbb{R}^n \to \mathbb{R}$ is the number of times we need to differentiate it along system dynamics (1) until any component of u explicitly shows in the corresponding derivative.

In this paper, a **safety requirement** is defined as $b(x,t) \ge 0$, and **safety** is the forward invariance of the set $\mathcal{C} := \{x \in \mathbb{R}^n : b(x,t) \ge 0\}$. The relative degree of time-varying function b is also referred to as the relative degree of safety requirement $b(x,t) \ge 0$. For $b(x,t) \ge 0$ with relative degree

 $m, b: \mathbb{R}^n \to \mathbb{R}$ and $\psi_0(\boldsymbol{x}, t) := b(\boldsymbol{x}, t)$, we define a sequence of functions $\psi_i: \mathbb{R}^n \to \mathbb{R}, i \in \{1, ..., m\}$ as

$$\psi_i(\mathbf{x},t) := \dot{\psi}_{i-1}(\mathbf{x},t) + \alpha_i(\psi_{i-1}(\mathbf{x},t)), \ i \in \{1,...,m\}, \ (4)$$

where $\alpha_i(\cdot)$, $i \in \{1,...,m\}$ denotes a $(m-i)^{th}$ order differentiable class κ function. A sequence of sets C_i are then defined based on (4) as

$$C_i := \{ x \in \mathbb{R}^n : \psi_{i-1}(x, t) > 0 \}, \ i \in \{1, ..., m\}.$$
 (5)

Definition 5 (Time-varying High Order Control Barrier Function (HOCBF) [10]). Let $\psi_i(\boldsymbol{x},t), i \in \{1,...,m\}$ be defined by (4) and $\mathcal{C}_i, i \in \{1,...,m\}$ be defined by (5). A function $b: \mathbb{R}^n \to \mathbb{R}$ is a time-varying High Order Control Barrier Function (HOCBF) with relative degree m for system (1) if there exist $(m-i)^{th}$ order differentiable class κ functions $\alpha_i, i \in \{1,...,m\}$ such that

$$\sup_{\boldsymbol{u}\in\mathcal{U}} [L_f^m b(\boldsymbol{x},t) + L_g L_f^{m-1} b(\boldsymbol{x},t) \boldsymbol{u} + \frac{\partial^m b(\boldsymbol{x},t)}{\partial t^m} + O(b(\boldsymbol{x},t)) + \alpha_m(\psi_{m-1}(\boldsymbol{x},t))] \ge 0,$$
(6)

 $\forall x \in \mathcal{C}_1 \cap, ..., \cap \mathcal{C}_m$.

In (6), L_f^m denote m-th order Lie derivatives along f; L_g is the Lie derivative along g. We use $O(\cdot) = \sum_{i=1}^{m-1} L_f^i(\alpha_{m-1} \circ \psi_{m-i-1})(\boldsymbol{x},t)$ and assume that $L_g L_f^{m-1} b(\boldsymbol{x},t) \boldsymbol{u} \neq 0$ on the boundary of set $\mathcal{C}_1 \cap, \ldots, \cap \mathcal{C}_m$.

Theorem 1 (Safety Guarantee [10]). Given a HOCBF b(x,t) from Def. 5 with corresponding sets C_0, \ldots, C_{m-1} defined by (5), if $\mathbf{x}(0) \in C_0 \cap \cdots \cap C_{m-1}$, then any Lipschitz controller \mathbf{u} that satisfies the inequality in (6), $\forall t \geq 0$ renders $C_0 \cap \cdots \cap C_{m-1}$ forward invariant for system (1), i.e., $\mathbf{x} \in C_0 \cap \cdots \cap C_{m-1}$, $\forall t \geq 0$.

The existing works [9], [10] leverage HOCBFs (6) to handle systems with high relative degree, combining them with quadratic cost functions to formulate safety-critical optimization-based controllers. In these frameworks, the continuous-time problem is discretized over sampling intervals $[t_k, t_{k+1})$, where the state $x(t_k)$ is measured and a quadratic program (QP) with HOCBF constraints is solved to obtain the optimal control $u^*(t_k)$, which is applied in a zero-order-hold (ZOH) manner while the system evolves according to (1). Because controller updates occur only at discrete sampling times, the system evolves open-loop between updates, potentially causing inter-sampling effects [30], where transient constraint violations arise even if the HOCBF conditions hold at the sampled instants. The severity of this effect depends on several factors, including the sampling period, the Lipschitz continuity of the system dynamics, and the steepness of the barrier functions. Specifically, when the sampling interval is not sufficiently small or the system exhibits fast dynamics, the state trajectory may temporarily exit the safe set between samples, leading to safety degradation despite satisfying the HOCBF constraints at discrete times.

III. PROBLEM FORMULATION AND APPROACH

The objective is to develop a control strategy for the system in (1) that ensures continuous-time reach-and-remain of a desired target within prescribed time horizons, minimizes energy consumption, guarantees continuous-time safety, and satisfies the input constraints (2).

Finite-Time Reach-and-Remain Requirement: Given time bounds $0 \le T_1 < T_2 \le \infty$, the state of system (1) is required to reach a closed set $S := \{x \in \mathbb{R}^n \mid h(x) \ge 0\}$, defined by a continuously differentiable function $h : \mathbb{R}^n \to \mathbb{R}$, within the horizon T_1 . That is, for a given initial condition $x(0) \in \mathbb{R}^n$, there must exist a time $t_r \in [0, T_1]$ such that $x(t_r) \in S$. Furthermore, after reaching the set, the state is required to remain in S for all subsequent times over the interval $[t_r, T_2]$, i.e., $x(t) \in S$ for all $t \in [t_r, T_2]$.

Safety Requirement: System (1) should always satisfy a safety requirement of the form:

$$b(\boldsymbol{x}(t)) \ge 0, \boldsymbol{x} \in \mathbb{R}^n, \forall t \in [0, T_2], \tag{7}$$

where $b:\mathbb{R}^n\to\mathbb{R}$ is assumed to be a continuously differentiable function.

Control Limitation Requirement: The controller u should always satisfy (2) for all $t \in [0, T_2]$.

A control policy is said to be **feasible** if all constraints arising from the aforementioned requirements are satisfied and remain mutually non-conflicting over the time interval $[0, T_2]$. In this paper, we consider the following problem:

Problem 1. Determine a feasible control policy for system (1) that minimizes the following cost:

$$J(\boldsymbol{u}(t)) = \int_0^{T_2} D(\|\boldsymbol{u}(t)\|) dt, \tag{8}$$

while satisfying all previously stated requirements.

In Eq. (8), $\|\cdot\|$ denotes the 2-norm of a vector and $D(\cdot)$ is a strictly increasing function of its argument. This problem setup is directly motivated by STL, as spatio-temporal STL specifications naturally reduce to finite-time reach-and-remain tasks. Therefore, solving Problem 1 directly enables satisfaction of this class of STL requirements.

As mentioned in Sec. II, when Problem 1 is reduced to a sequence of QPs and solved at discrete time steps, the corresponding discretization introduces inter-sampling effects, where the control input is held constant in a ZOH manner between updates and the system evolves open-loop, potentially leading to transient requirement violations. Existing sampled-data CBF formulations that address inter-sampling issues cannot effectively handle time-varying or high-order CBFs, and when multiple CBF constraints are enforced simultaneously, the tightened inequalities may conflict, leading to infeasibility of the optimization problem. These limitations motivate the development of new formulations that can maintain continuous-time safety, reach-and-remain and feasibility for time-varying high-order CBFs under sampled implementations.

Approach: In this paper, we introduce Sampling-Aware Control Barrier Functions (SACBFs) that explicitly address

both the inter-sampling and high relative degree issues. By incorporating Taylor-based upper bounds on the barrier function's evolution between sampling instants, SACBFs ensure continuous-time forward invariance of corresponding sets under ZOH control. Moreover, a relaxation variable is added to each SACBF constraint to improve feasibility when multiple SACBFs are jointly used to enforce the desired requirements.

IV. SAMPLING-AWARE CONTROL BARRIER FUNCTIONS

In this section, we develop the framework of Sampling-Aware Control Barrier Functions (SACBFs), which systematically accounts for inter-sampling effects and high relative degree constraints to ensure continuous-time forward invariance of desired sets under ZOH control.

A. Sampling-Aware Control Barrier Functions

Let the sampling period be $\Delta t > 0$, and consider the affine control system (1) evolving on a compact set \mathcal{X} , where the control input $u \in \mathcal{U}$ is held constant within each sampling interval $[t_k, t_{k+1})$ under a ZOH implementation, i.e.,

$$\boldsymbol{u}(t) = \boldsymbol{u}(t_k), \quad t \in [t_k, t_{k+1}). \tag{9}$$

Consider functions $\psi_i(\boldsymbol{x},t)$ defined in (4), where each α_i is defined as $\alpha_i(\psi_{i-1}(\boldsymbol{x},t)) = \lambda_i\psi_{i-1}(\boldsymbol{x},t)^{\eta_i}$ for some $\lambda_i,\eta_i>0$. Integrating $\dot{\psi}_{m-1}(\boldsymbol{x},t)\geq -\lambda_m\psi_{m-1}(\boldsymbol{x},t)^{\eta_m}$ and using the comparison lemma in [29], we have

$$\psi_{m-1}(\boldsymbol{x}(t),t) \ge \psi_{m-1}(\boldsymbol{x}(t_0),t_0) e^{-\lambda_m (t-t_0)}, \eta_i = 1,$$

$$\psi_{m-1}(\boldsymbol{x}(t),t) \ge \left[\psi_{m-1}(\boldsymbol{x}(t_0),t_0)^{1-\eta_m} - \right]$$

$$\lambda_m (1-\eta_m) (t-t_0) \Big]_+^{\frac{1}{1-\eta_m}}, \eta_i \ne 1,$$
(10)

where $[a]_+ := \max\{a, 0\}$. From the above expression, it can be seen that the right-hand side of the inequality is always nonnegative if $\psi_{m-1}(\boldsymbol{x}(t_0), t_0) \geq 0$. Therefore, Eq. (10) can be compactly represented as follows:

$$\psi_{m-1}(\boldsymbol{x}(t),t) \ge \mathcal{L}(\psi_{m-1}(\boldsymbol{x}(0),0),\lambda_m,\eta_m,t-t_0) \ge 0,$$
(11)

where $\psi_{m-1}(\boldsymbol{x}(0),0) \geq 0, \lambda_m > 0, \eta_m > 0$. For notational simplicity, we denote $\psi_{m-1}(t) \Longleftrightarrow \psi_{m-1}(\boldsymbol{x}(t),t), \mathcal{L}(t_0,t-t_0) \Longleftrightarrow \mathcal{L}(\psi_{m-1}(\boldsymbol{x}(0),0),\lambda_m,\eta_m,t-t_0)$ and the same convention is used hereafter. For the interval $[t_k,t_{k+1})$ starting from t_k , based on (11), we have

$$\psi_{m-1}(t_k + \Delta t) > \mathcal{L}(t_k, \Delta t) > 0. \tag{12}$$

Expanding $\psi_{m-1}(t_k+\Delta t)$ around t_k up to the second order using a Taylor-based expansion yields

$$\psi_{m-1}(t_k + \Delta t) = \psi_{m-1}(t_k) + \Delta t \dot{\psi}_{m-1}(t_k) + \frac{(\Delta t)^2}{2} \ddot{\psi}_{m-1}(\xi),$$
(13)

where $\xi \in [t_k, t_k + \Delta t]$ is some intermediate time, and the last term in the above corresponds to the Lagrange remainder. To

calculate $\ddot{\psi}_{m-1}(\xi)$, we apply the chain rule of differentiation along dynamic system (1) and obtain

$$\ddot{\psi}_{m-1}(t) = \dot{\boldsymbol{x}}^{\top} (\nabla_{\boldsymbol{x}}^{2} \psi_{m-1}(t)) \dot{\boldsymbol{x}} + \nabla_{\boldsymbol{x}} \psi_{m-1}(t)^{\top} \Big(f_{\boldsymbol{x}} \dot{\boldsymbol{x}} + g_{\boldsymbol{x}} \dot{\boldsymbol{x}} u + f_{t} + g_{t} \boldsymbol{u} + g(\boldsymbol{x}, t) \boldsymbol{u} \Big) + 2 \nabla_{\boldsymbol{x}t}^{2} \psi_{m-1}(t)^{\top} \dot{\boldsymbol{x}}$$

$$+ \nabla_{tt}^{2} \psi_{m-1}(t),$$

$$(14)$$

where $f_{\boldsymbol{x}} \coloneqq \frac{\partial f}{\partial \boldsymbol{x}}(\boldsymbol{x},t), \ f_{t} \coloneqq \frac{\partial f}{\partial t}(\boldsymbol{x},t), \ g_{\boldsymbol{x}} \coloneqq \frac{\partial g}{\partial \boldsymbol{x}}(\boldsymbol{x},t), \ g_{t} \coloneqq \frac{\partial g}{\partial t}(\boldsymbol{x},t), \ \nabla_{\boldsymbol{x}}\psi_{m-1}(t) \coloneqq \frac{\partial}{\partial \boldsymbol{x}}(\psi_{m-1}(\boldsymbol{x},t)), \ \nabla_{\boldsymbol{x}}^{2}\psi_{m-1}(t) \ \coloneqq \frac{\partial}{\partial \boldsymbol{x}}(\nabla_{\boldsymbol{x}}\psi_{m-1}(t)), \ \nabla_{\boldsymbol{x}}^{2}\psi_{m-1}(t) \ \coloneqq \frac{\partial}{\partial t}(\nabla_{\boldsymbol{x}}\psi_{m-1}(t)), \ \nabla_{tt}^{2}\psi_{m-1}(t) \ \coloneqq \frac{\partial^{2}\psi_{m-1}(t)}{\partial t^{2}}, \ \dot{\boldsymbol{u}} = \boldsymbol{0}. \ \text{In} \ (14), \ \text{the arguments} \ \boldsymbol{x}(t) \ \text{and} \ \boldsymbol{u}(t) \ \text{in} \ \psi_{m-1}(t) \ \text{are omitted} \ \text{for notational simplicity.} \ \text{Because} \ f, \ g, \ \text{and} \ \psi_{m-1} \ \text{are continuously differentiable} \ \text{and the system trajectory} \ \boldsymbol{x}(t) \ \text{evolves} \ \text{within a compact set} \ \mathcal{X}, \ \text{all terms in} \ (14) \ \text{are continuous with respect to} \ t. \ \text{Hence}, \ \ddot{\psi}_{m-1}(t) \ \text{is continuous} \ \text{on the closed interval} \ [t_{k}, t_{k} + \Delta t]. \ \text{By the extreme value} \ \text{theorem in} \ [31], \ \text{there exists a finite constant} \ \bar{M}_{k} > 0 \ \text{such} \ \text{that} \ |\ddot{\psi}_{m-1}(t)| \leq \bar{M}_{k}, \forall \ t \in [t_{k}, t_{k} + \Delta t].$

Definition 6 (Sampling-Aware Control Barrier Function (SACBF)). Let $\psi_i(\boldsymbol{x},t), i \in \{1,\ldots,m\}$ be defined by (4), $\mathcal{C}_i, i \in \{1,\ldots,m\}$ be defined by (5) and $\mathcal{L}(t_k,\Delta t)$ be defined by (10), (11). Consider the affine control system (1), which evolves within a compact set $\mathcal{X} \subset \mathbb{R}^n$, where the control input $\boldsymbol{u}(t)$ is held constant, i.e., $\boldsymbol{u}(t) = \boldsymbol{u}(t_k)$ for $t \in [t_k, t_k + \Delta t), k \in \{0, 1, \ldots\}$ under a zero-order-hold (ZOH) implementation. A function $b: \mathbb{R}^n \to \mathbb{R}$ is called a Sampling-Aware Control Barrier Function (SACBF) with relative degree m for system (1) if there exist $(m-i)^{\text{th}}$ -order differentiable class- κ functions $\alpha_i(\psi_{i-1}(\boldsymbol{x},t)) = \lambda_i \psi_{i-1}(\boldsymbol{x},t)^{\eta_i}$, with $\lambda_i > 0$ and $\eta_i > 0$, $i \in \{1,\ldots,m\}$, such that

$$L_{f}\psi_{m-1}(t_{k}) + L_{g}\psi_{m-1}(t_{k})\boldsymbol{u} + \frac{\partial\psi_{m-1}(t_{k})}{\partial t} \geq \frac{\mathcal{L}(t_{k}, \Delta t) - \psi_{m-1}(t_{k})}{\Delta t} + \frac{1}{2}\bar{M}_{k}\Delta t,$$

$$(15)$$

 $\forall x \in \mathcal{C}_1 \cap, ..., \cap \mathcal{C}_m$. $\bar{M}_k > 0$ denotes the upper bound of the second derivative term (i.e., $|\ddot{\psi}_{m-1}(t)|$ in (13)) over the sampling interval $[t_k, t_k + \Delta t]$.

Theorem 2. Given a SACBF b(x) as defined in Def. 6, with the associated sets C_0, \ldots, C_{m-1} defined by (5), suppose the initial condition satisfies $x(t_0) \in C_0 \cap \cdots \cap C_{m-1}$. Then, under ZOH control with sampling period $\Delta t > 0$, any locally Lipschitz controller u(t) that satisfies the SACBF inequality (15) for all $t \geq 0$ renders the set $C_0 \cap \cdots \cap C_{m-1}$ forward invariant for the system (1), i.e., $x \in C_0 \cap \cdots \cap C_{m-1}$, $\forall t \geq 0$.

Proof. Starting from the initial time interval $[t_0, t_0 + \Delta t]$, by combining Eqs. (12), (13) and $\ddot{\psi}_{m-1}(\xi) \geq -\bar{M}_0$, we obtain

$$\psi_{m-1}(t_0 + \Delta t) \ge \psi_{m-1}(t_0) + \Delta t \dot{\psi}_{m-1}(t_0) - \frac{(\Delta t)^2}{2} \bar{M}_0$$

$$\ge \mathcal{L}(t_0, \Delta t) \ge 0.$$
(16)

Substitute $\dot{\psi}_{m-1}(t_0) = L_f \psi_{m-1}(t_0) + L_g \psi_{m-1}(t_0) u + \frac{\partial \psi_{m-1}(t_0)}{\partial t}$ into (16), we have the same inequality as (15), this indicates that satisfying inequality (15) guarantees the nonnegativity of $\psi_{m-1}(t_0 + \Delta t)$ at the end of the sampling interval. Let $\tau \in [0, \Delta t]$, we want

$$\psi_{m-1}(t_0 + \tau) \ge \psi_{m-1}(t_0) + \tau \dot{\psi}_{m-1}(t_0) - \frac{\tau^2}{2} \bar{M}_0 \ge 0.$$
(17)

Based on (15), we have

$$\dot{\psi}_{m-1}(t_0) \ge \frac{\mathcal{L}(t_0, \Delta t) - \psi_{m-1}(t_0)}{\Delta t} + \frac{1}{2}\bar{M}_0 \Delta t.$$
 (18)

Substituting (18) into (17), we want

$$\psi_{m-1}(t_0 + \tau) \ge l(\tau) = \psi_{m-1}(t_0) + \tau \left(\frac{\mathcal{L}(t_0, \Delta t) - \psi_{m-1}(t_0)}{\Delta t} + \frac{1}{2}\bar{M}_0 \Delta t\right) - \frac{1}{2}\bar{M}_0 \tau^2 \ge 0.$$
(19)

Define $A=\frac{\mathcal{L}(t_0,\triangle t)-\psi_{m-1}(t_0)}{\Delta t}, B=\frac{1}{2}\bar{M}_0\Delta t$. The function $l(\tau)$ is a quadratic function of τ that opens downward. We assume that Δt is larger than its largest root, as given below:

$$\Delta t > \frac{-(A+B) - \sqrt{(A+B)^2 + 2\bar{M}_0\psi_{m-1}(t_0)}}{-\bar{M}_0}.$$
 (20)

By rewriting (20), we have

$$-\bar{M}_0 \Delta t + A + B = A - B < -\sqrt{(A+B)^2 + 2\bar{M}_0 \psi_{m-1}(t_0)},$$
(21)

where $\psi_{m-1}(t_0) \geq 0$. Following the above equation, we have that $A-B \leq 0$, then we square both sides of inequality (21) to obtain $(A-B)^2 \geq (A+B)^2 + 2\bar{M}_0\psi_{m-1}(t_0)$. Rearranging terms gives $-2AB \geq \bar{M}_0\psi_{m-1}(t_0)$. Substituting A and B into this inequality, we have $\bar{M}_0\mathcal{L}(t_0,\Delta t) \leq 0$. However, since $\bar{M}_0\mathcal{L}(t_0,\Delta t) \geq 0$ clearly holds, the assumption (20) is invalid, and therefore Δt must be less than or equal to the larger root of the quadratic function $l(\tau)$. Consequently, since the quadratic function $l(\tau)$ remains nonnegative for all $\tau \in [0,\Delta t]$ as long as Δt does not exceed its larger root, ensuring that Δt is less than or equal to the larger root of $l(\tau)$ guarantees that $l(\tau) \geq 0$ holds throughout the interval. Therefore, satisfying inequality (15) ensures that $\psi_{m-1}(t_0+\tau)$ remains nonnegative for all $\tau \in [0,\Delta t]$.

We now have proved that $\psi_{m-1}(t) \geq 0, \forall t \in [t_0, t_0 + \Delta t]$. By shifting the time interval to $[t_1, t_1 + \Delta t]$ and repeating the same proof, we obtain $\psi_{m-1}(t) \geq 0, \forall t \in [t_1, t_1 + \Delta t]$. By iterating this process, it follows that $\psi_{m-1}(t) \geq 0$ for all $t \geq 0$. With this result and by following the safety guarantee proof of HOCBFs in [10], we can further derive $\psi_{m-2}(t) \geq 0, \ldots, \psi_0(t) = b(\boldsymbol{x}, t) \geq 0$. Therefore, the intersection of the sets $\mathcal{C}_0, \ldots, \mathcal{C}_{m-1}$ is forward invariant.

Remark 1. To simplify the computation, in Eq. (10) and Def. 6, we define the class κ functions in the form $\alpha_i(\psi_{i-1}(\boldsymbol{x},t)) = \lambda_i \psi_{i-1}(\boldsymbol{x},t)^{\eta_i}$. However, the definition of a class K function can be made more general, for example, by defining it as a polynomial function of $\psi_{i-1}(\boldsymbol{x},t)$. As long as all coefficients and exponents of the polynomial are positive, the Def. 6 and Thm. 2 of SACBFs remain valid.

Since Eq. (15) serves as a constraint for solving the optimal input, it may conflict with the input bounds (2) or other SACBF constraints, resulting in infeasibility. Hence, a relaxation variable is added to improve feasibility without compromising the forward invariance guarantee of the desired set. In Eq. (12), we add a slack variable ω and obtain

$$\psi_{m-1}(t_k + \Delta t) > \omega_k \mathcal{L}(t_k, \Delta t) > 0, \tag{22}$$

where $\omega_k \geq 0$. Due to the modification in Eq. (22), the corresponding term $\mathcal{L}(t_k, \Delta t)$ in Eq. (15) is replaced by $\omega_k \mathcal{L}(t_k, \Delta t)$. The slack variable ω is typically assigned a reference value of 1 by adding a weight scalar q>0 to the quadratic penalty $(\omega-1)^2$ in the cost function (8), thereby ensuring that Eqs. (22) and (15) remain unchanged under nominal conditions. When no input can satisfy the SACBF constraint (15), ω is allowed to decrease within the range [0,1] to relax the constraint and enhance feasibility. Moreover, since $\omega_k \mathcal{L}(t_k, \Delta t) \geq 0$, introducing the slack variable does not affect the non-negativity of $\psi_{m-1}(t_k + \Delta t)$. Therefore, this relaxation enhances feasibility without compromising the forward invariance guarantee.

C. Estimation of the Taylor-Based Upper Bound

For notational simplicity, we define $F:=f+g\,u$, which represents the affine vector field under a fixed control input u. Then, the instantaneous bound of $|\dot{\psi}_{m-1}(t)|$ in (13) can be written as

$$\Phi := \|\nabla_{\boldsymbol{x}}^{2} \psi_{m-1} \| \|F\|^{2} + \|\nabla_{\boldsymbol{x}} \psi_{m-1} \| (\|f_{\boldsymbol{x}}\| + \|g_{\boldsymbol{x}}\| \|\boldsymbol{u}\|) \|F\|
+ 2 \|\nabla_{\boldsymbol{x}t}^{2} \psi_{m-1} \| \|F\| + \|\nabla_{tt}^{2} \psi_{m-1} \|
+ \|\nabla_{\boldsymbol{x}} \psi_{m-1} \| (\|f_{t}\| + \|g_{t}\| \|\boldsymbol{u}\|).$$
(23)

This follows from taking the norm of each term in $\ddot{\psi}_{m-1}(t)$ and applying the triangle inequality. To avoid taking a conservative supremum over the entire state space \mathcal{X} , we restrict the evaluation to a local trajectory tube

$$\mathcal{R}_k(\Delta t) := \left\{ \boldsymbol{x} : \|\boldsymbol{x} - \boldsymbol{x}(t_k)\| \le \rho(\Delta t) \right\},$$

$$\rho(\Delta t) := \frac{e^{L_F \Delta t} - 1}{L_F} \|F(\boldsymbol{x}(t_k), \boldsymbol{u})\|,$$
(24)

where L_F is the local Lipschitz constant of $F(\cdot)$ with respect to \boldsymbol{x} uniformly over $t \in [t_k, t_k + \Delta t]$. If $L_F = 0$, then $\rho(\Delta t) = \Delta t \|F(\boldsymbol{x}(t_k), \boldsymbol{u})\|$. This local trajectory tube bound follows from the L_F and the integral form of Grönwall's inequality [29]. The local Taylor-based upper bound is therefore defined as

$$\bar{M}_{k}(\Delta t) := \sup_{\substack{t \in [t_{k}, t_{k} + \Delta t] \\ (\boldsymbol{x}, \boldsymbol{u}) \in \mathcal{R}_{k}(\Delta t) \times \mathcal{U}}} \Phi(\boldsymbol{x}, \boldsymbol{u}, t), \tag{25}$$

$$|\ddot{\psi}_{m-1}(t)| \leq \bar{M}_k(\Delta t), \quad \forall t \in [t_k, t_k + \Delta t].$$

Computational Approximation: When evaluating $\bar{M}_k(\Delta t)$ exactly is computationally expensive, we approximate it using r sample points based on the Gauss–Legendre nodes [32]:

$$\hat{M}_k := \max_{i=1,\dots,r} \Phi(\boldsymbol{x}_i, \boldsymbol{u}_i, t_i), \ t_i = t_k + \gamma_i \Delta t,$$

$$\boldsymbol{x}_i \approx \boldsymbol{x}(t_i), \ \boldsymbol{u}_i \approx \boldsymbol{u}(t_i),$$
(26)

and

$$\bar{M}_k(\Delta t) \leq \hat{M}_k + L_{\Phi}(\Delta_x + \Delta_u),$$
 (27)

where $\{\gamma_i\}$ are the r-point Gauss–Legendre quadrature nodes (r=3-5), $\Delta_{\boldsymbol{x}}$ and $\Delta_{\boldsymbol{u}}$ denote the maximum variations of the state and control between adjacent nodes (approximately $\frac{\rho(\Delta t)}{2}$ and $\frac{|\boldsymbol{u}_{i+1}-\boldsymbol{u}_i|}{2}$, respectively), and L_{Φ} is the local Lipschitz constant of Φ with respect to both \boldsymbol{x} and \boldsymbol{u} . Gauss–Legendre nodes provide good coverage of smooth functions on a finite interval, so \hat{M}_k offers a tight and tractable estimate of the local supremum.

D. SACBFs Design for Safety and Finite-Time Reach-and-Remain

To formalize the safety and finite-time reach-and-remain requirements, we define two candidate SACBF formulations based on selected state components.

For the **safety requirement**, we specify the states $x_{i,s} \in \mathbb{R}^{n_i}$ that must remain within a fixed safe region centered at x_{i,s_0} with a constant boundary radius $r_{i,s_0} > 0$. The corresponding constraint is

$$\psi_{i,0}^{s}(\boldsymbol{x}_{i,s}) = b_{i}(\boldsymbol{x}_{i,s}) = \|\boldsymbol{x}_{i,s} - \boldsymbol{x}_{i,s_{0}}\|_{\bar{p}_{i}} - r_{i,s_{0}}^{\bar{p}_{i}} \ge 0, \quad (28)$$

where $x_{i,s_0} \in \mathbb{R}^{n_i}$, $n_i \leq n$, and $\|\cdot\|_{\bar{p}_i}$ denotes the \bar{p}_i -norm. Here, the index i denotes the i-th safety requirement.

For the **finite-time reach-and-remain requirement**, we define the states $x_{j,c} \in \mathbb{R}^{n_j}$ that must reach a target region centered at x_{j,c_d} with a constant boundary radius $\varepsilon_{j,c_d} > 0$ within the finite time horizon $[T_{j,c_0}, T_{j,c_1}]$ by satisfying

$$\psi_{j,0}^{c}(\boldsymbol{x}_{j,c},t) = h_{j}(\boldsymbol{x}_{j,c},t) = \varepsilon_{j}(t)^{\bar{p}_{j}} - \|\boldsymbol{x}_{j,c} - \boldsymbol{x}_{j,c_{d}}\|_{\bar{p}_{j}} \ge 0,$$
(29)

where $x_{j,c_d} \in \mathbb{R}^{n_j}$, $n_j \leq n$, and $\|\cdot\|_{\bar{p}_j}$ denotes the \bar{p}_j -norm. The function $\varepsilon_j(t)$ specifies a contracting convergence radius:

$$\varepsilon_j(t) = \varepsilon_{j,c_0} - K_{j,c}(t - T_{j,c_0}), \quad K_{j,c} = \frac{\varepsilon_{j,c_0} - \varepsilon_{j,c_d}}{T_{j,c_1} - T_{j,c_0}},$$
 (30)

with $\varepsilon_{j,c_0} \geq \varepsilon_{j,c_d} \geq 0$. Here, the index j denotes the j-th reachability requirement. $K_{j,c}$ denotes the contraction rate of the convergence boundary, with ε_{j,c_0} specifying the initial radii. The state $x_{j,c}$ is always contained within the region defined by $\varepsilon_j(t)$. As $\varepsilon_j(t)$ gradually decreases, the state progressively converges until it reaches the target region within the specified time horizon. For the "remain" requirement that the state remains within the radius ε_{j,c_d} over the interval $[T_{j,c_1},T_{j,c_2}]$, we set $\varepsilon_{j,c_0}=\varepsilon_{j,c_d}$ and $K_{j,c}=0$ for the time horizon $[T_{j,c_1},T_{j,c_2}]$. In this case, the radius remains constant, and the SACBF enforces that the state remains within this fixed region throughout the interval.

E. Computational Complexity

The computational burden of solving Problem 1 is dominated by the SACBF-QP solved at each sampling instant. With q decision variables and N constraints, the QP has a worst-case complexity of $\mathcal{O}((q+N)^3)$. The additional SACBF overhead arises from evaluating the Taylor-based upper bound $\bar{M}_k(\Delta t)$ in (25), which depends on the expression of Φ

in (23). Since \bar{M}_k is approximated using only r Gauss–Legendre nodes, this step scales linearly as $\mathcal{O}(r\,C_\Phi)$, where C_Φ is the cost of evaluating Φ . Therefore, the overall per-step complexity is the sum of the QP complexity and the bound approximation, but it is empirically dominated by QP.

V. CASE STUDIES

In this section, we consider a unicycle with dynamics described by:

$$\underbrace{\begin{bmatrix} \dot{x}(t) \\ \dot{y}(t) \\ \dot{\theta}(t) \\ \dot{v}(t) \end{bmatrix}}_{\dot{x}(t)} = \underbrace{\begin{bmatrix} v(t)\cos(\theta(t)) \\ v(t)\sin(\theta(t)) \\ 0 \\ 0 \end{bmatrix}}_{f(\boldsymbol{x}(t))} + \underbrace{\begin{bmatrix} 0 & 0 \\ 0 & 0 \\ 1 & 0 \\ 0 & 1 \end{bmatrix}}_{g(\boldsymbol{x}(t))} \underbrace{\begin{bmatrix} u_1(t) \\ u_2(t) \end{bmatrix}}_{\boldsymbol{u}(t)}, \quad (31)$$

which is of the form (1). In (31), $[x, y]^{\top}$ denote the coordinates of the unicycle, v is its linear speed, θ denotes the heading angle, and \mathbf{u} represent the angular velocity (u_1) and linear acceleration (u_2) , respectively. The input bounds are defined as $\mathcal{U} = \{\mathbf{u}_t \in \mathbb{R}^2 : -10 \cdot \mathcal{I}_{2 \times 1} \leq \mathbf{u} \leq 10 \cdot \mathcal{I}_{2 \times 1}\}$.

The QP at each time step is solved using MATLAB's quadprog, and the system dynamics are integrated with the ode 45 solver. All simulations are carried out on a computer with an Intel[®] CoreTM i7-11750F CPU running at 2.50GHz.

A. Safety Requirement

For the safety requirement, we consider N_s circular obstacles that the robot must avoid, indexed by $i \in \{1,...,N_s\}$. The safety boundary is constructed from a quadratic distance function defined as

$$b_i(\boldsymbol{x}_{i,s}) = (x - x_{i,s_0})^2 + (y - y_{i,s_0})^2 - r_{i,s_0}^2,$$
 (32)

where (x_{i,s_0}, y_{i,s_0}) and r_{i,s_0} denote the center coordinates and radius of the *i*-th obstacle, respectively. Based on (28), we define SACBF as

$$\psi_{i,0}^s(\boldsymbol{x}_{i,s}) = b_i(\boldsymbol{x}_{i,s}). \tag{33}$$

B. Finite-Time Reach-and-Remain Requirement

The finite-time reach-and-remain requirement specifies that the system must reach a set of circular target regions, indexed by $j \in \{1,...,N_c\}$, and then remain within them. The boundary of the j-th desired region is constructed from a quadratic distance function defined as

$$h_j(\mathbf{x}_{j,c}) = \varepsilon_{j,c_d}^2 - (x - x_{j,c_d})^2 - (y - y_{j,c_d})^2,$$
 (34)

where (x_{j,c_d}, y_{j,c_d}) and ε_{j,c_d} denote the center coordinates and radius of the *j*-th target area, respectively. Based on (29), (30), we define SACBF as

$$\psi_{j,0}^{c}(\boldsymbol{x}_{j,s},t) = \varepsilon_{j,c_0}^{2} - K_{j,c}(t - T_{j,c_0}) - (x - x_{j,c_d})^{2} - (y - y_{j,c_d})^{2}, K_{j,c} = \frac{\varepsilon_{j,c_0}^{2} - \varepsilon_{j,c_d}^{2}}{T_{j,c_1} - T_{j,c_0}}.$$
(35)

Here, ε_{j,c_0} is the initial radius of the circular region containing the robot at time T_{j,c_0} , and $K_{j,c}$ specifies the linear shrinking rate that decreases the radius from ε_{j,c_0} to ε_{j,c_d} over $[T_{j,c_0},T_{j,c_1}]$. This yields a time-varying boundary that

contracts toward the j-th target region, ensuring finite-time reachability. If the robot is required to remain within this region over $[T_{j,c_1},T_{j,c_2}]$, we set $\varepsilon_{j,c_0}=\varepsilon_{j,c_d}$ and $K_{j,c}=0$ in (35) for that interval.

C. Complete Cost Function for SACBF-QP

By formulating the constraints from the SACBFs in (15), which are constructed based on (33) and (35) (with relative degree 2), together with the input bounds (2), we can define the cost function for QP as

$$\min_{\boldsymbol{u}(t),\omega_k(t)} \int_0^T [\boldsymbol{u}(t)^{\top} \boldsymbol{u}(t) + \sum_{k=1}^{N_s + N_c} q_k (\omega_k(t) - 1)^2] dt, \quad (36)$$

where ω_k is a relaxation variable introduced in the SACBF constraint (22), q_k is a positive weight scalar, and the slack variable ω_k is designed to converge to 1. Since existing approaches that address the inter-sampling issue cannot handle high-order constraints, the HOCBF framework (6) is selected as the benchmark for comparison. The proposed method without the slack variable is denoted as SACBF, while the one incorporating the relaxation variable is referred to as the relaxed SACBF (r-SACBF). All methods are implemented with identical hyperparameters for a fair comparison.

D. Case Study I

Consider a case where the robot must avoid a circular obstacle centered at (0,0) with a radius of 1, while reaching a circular target region centered at (3,0) with a radius of 1 within 5 seconds. The robot starts from the initial position (-3,0) with an initial speed of 1. The hyperparameters are set as $\lambda_k=2$, $\eta_k=1$, $q_k=200$, r=5, $\varepsilon_{1,c_0}=7$, $T_{1,c_1}=5$, $T_{1,c_0}=0$, and $\Delta t=0.1$.

As shown in Fig. 2, a smaller initial heading angle makes it more difficult for the robot to satisfy the safety requirement. The constraint in (33) enforces safety by steering the robot away from obstacles, while the constraint in (35) enforces finite-time reachability by driving it toward the target region. Since the robot's initial position, the obstacle center, and the target center are collinear, a smaller heading angle (i.e., the initial velocity points more directly toward the obstacle) intensifies the conflict between safety and reachability. This increased conflict may lead to unsafe behaviors or even infeasibility of the optimization problem. Due to the intersampling issue, the HOCBF method becomes unsafe when the initial heading angles are 0 or $\frac{\pi}{12}$, as the robot crosses the obstacle boundary. In contrast, the SACBF and r-SACBF methods maintain safety under the same conditions. The SACBF method incorporates a Taylor-based upper bound to address the inter-sampling issue, which reduces the feasible space of the control input and makes infeasibility more likely compared to HOCBF. Consequently, when the initial heading angles are 0 or $\frac{\pi}{12}$, the SACBF method becomes infeasible due to overly restrictive safety constraints, whereas for initial heading angles of $\frac{\pi}{6}$ or $\frac{\pi}{2}$, infeasibility arises from excessively tight reachability constraints. Meanwhile, the r-SACBF method achieves safe and successful convergence to the desired region for all tested initial heading angles.

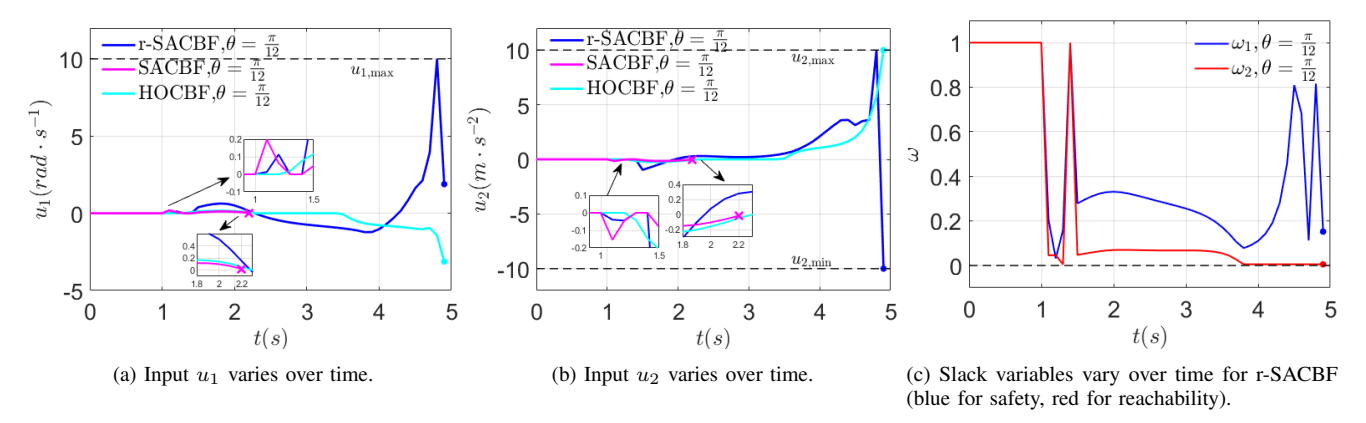


Fig. 1: Time evolution of decision variables under r-SACBF, SACBF, and HOCBF methods when initial heading angle is $\frac{\pi}{12}$. The cross symbol "×" indicates that the QP is infeasible at that time step.

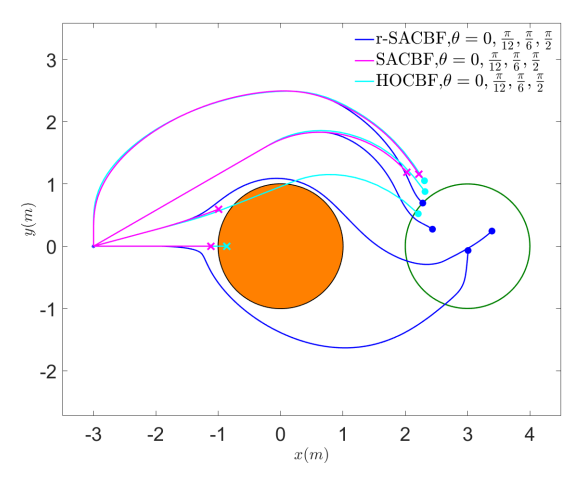


Fig. 2: Closed-loop trajectories with controllers derived using r-SACBF (blue), SACBF (magenta) and HOCBF (cyan) with different initial heading angle. The cross symbol "×" indicates that the QP is infeasible at that location.

Fig. 1 illustrates the time evolution of the decision variables when the initial heading angle is $\frac{\pi}{12}$. From Figs. 1a and 1b, it can be observed that the control inputs of the r-SACBF and SACBF methods respond earlier than those of the HOCBF method to satisfy the safety and reachability constraints. Moreover, due to the introduction of relaxation variables, the r-SACBF method avoids infeasibility. As shown in Fig. 1c, the relaxation variables decrease toward zero when the corresponding constraints become tight, thereby enhancing feasibility, which is consistent with the description provided in Sec. IV-B.

E. Case Study II

In this case, we consider a more complex task to evaluate the performance of the r-SACBF method under multiple constraints. The robot is required to avoid three circular obstacles with radii of 1, 2, and 1.5, centered at (0,0), (8,0), and (3,3), respectively. The mission specifies that the robot must reach desired region 1 (centered at (3,0) with a radius of 1) within 5 seconds, remain inside this region for the

following 7 seconds, then reach region 2 (centered at (0,7) with a radius of 0.5) within the next 6 seconds, and finally reach region 3 (centered at (4,5) with a radius of 0.2) within the subsequent 4 seconds. The robot starts from the initial position (-3,0) with an initial speed of 1 and an initial heading angle of $\frac{\pi}{6}$. The hyperparameters are set as $\lambda_k=2$, $\eta_k=1,\ q_k=1,\ r=5,\ \varepsilon_{1,c_0}=7,\ T_{1,c_2}=12,\ T_{1,c_1}=5,\ T_{1,c_0}=0,\ \varepsilon_{2,c_0}=9,\ T_{2,c_1}=18,\ T_{2,c_0}=12,\ \varepsilon_{3,c_0}=6,\ T_{3,c_1}=22,\ T_{3,c_0}=18$ and $\Delta t=0.1$.

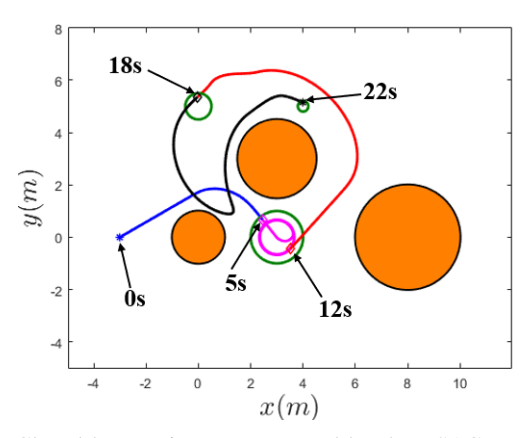


Fig. 3: Closed-loop trajectory generated by the r-SACBF method for the multi-constraint task. The robot avoids three obstacles and reaches the target regions at 5s, 18s, and 22s as indicated.

Fig. 3 shows the robot trajectory from 0s to 22s under the r-SACBF framework. As illustrated by the color-coded trajectories corresponding to different time intervals, the robot remains feasible throughout the task despite the presence of multiple constraints (three safety constraints, one reach-andremain constraint, and one input bound). In particular, as the target region gradually shrinks, the robot is still able to reach it within the required time, demonstrating the effectiveness and flexibility of the r-SACBF in handling complex, multi-constraint tasks. Fig. 4 illustrates the time evolution of the SACBF functions. Since the SACBFs have a relative degree of 2 with respect to system (31), both the zero-order SACBFs and the first-order SACBFs are shown. It can be observed

that, under the enforcement of (15), all functions remain positive within the 22s horizon, indicating that both safety and reach-and-remain requirements are satisfied.

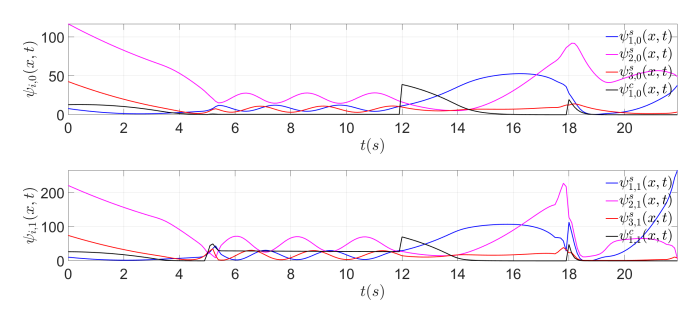


Fig. 4: Time evolution of the SACBF functions. The top plot shows the zero-order SACBFs, and the bottom plot shows the first-order SACBFs. The four curves correspond to three safety constraints (blue, magenta, red) and one reach-and-remain constraint (black). All functions stay positive over the 22s horizon.

VI. CONCLUSION AND FUTURE WORK

This paper introduced Sampling-Aware Control Barrier Functions (SACBFs) to ensure safety and finite-time reachand-remain for nonlinear systems with high relative-degree constraints under sampled implementations. By incorporating Taylor-based upper bounds, the SACBF framework explicitly captures inter-sampling effects and guarantees continuoustime forward invariance of the desired sets under zero-orderhold control. The introduction of relaxation variables further improves feasibility when multiple constraints are jointly enforced. Simulation studies on a unicycle robot validated the effectiveness and flexibility of the proposed approach, demonstrating safe and feasible performance in complex multi-constraint scenarios where conventional HOCBF-based methods fail. Future work will focus on extending SACBFs to systems with stochastic disturbances and model uncertainties, and integrating learning-based techniques for adaptive estimation of the Taylor-based upper bounds to further reduce conservatism and improve real-time scalability.

REFERENCES

- [1] S. Boyd, S. P. Boyd, and L. Vandenberghe, *Convex optimization*. Cambridge university press, 2004.
- [2] K. P. Tee, S. S. Ge, and E. H. Tay, "Barrier Lyapunov functions for the control of output-constrained nonlinear systems," *Automatica*, vol. 45, no. 4, pp. 918–927, 2009.
- [3] J.-P. Aubin, A. M. Bayen, and P. Saint-Pierre, Viability theory: new directions. Springer Science & Business Media, 2011.
- [4] S. Prajna, A. Jadbabaie, and G. J. Pappas, "A framework for worst-case and stochastic safety verification using barrier certificates," *IEEE Transactions on Automatic Control*, vol. 52, no. 8, pp. 1415–1428, 2007.
- [5] L. Wang, A. D. Ames, and M. Egerstedt, "Safety barrier certificates for collisions-free multirobot systems," *IEEE Transactions on Robotics*, vol. 33, no. 3, pp. 661–674, 2017.
- [6] P. Glotfelter, J. Cortés, and M. Egerstedt, "Nonsmooth barrier functions with applications to multi-robot systems," *IEEE control systems letters*, vol. 1, no. 2, pp. 310–315, 2017.
- [7] A. D. Ames, X. Xu, J. W. Grizzle, and P. Tabuada, "Control barrier function based quadratic programs for safety critical systems," *IEEE Transactions on Automatic Control*, vol. 62, no. 8, pp. 3861–3876, 2016.

- [8] A. D. Ames, K. Galloway, and J. W. Grizzle, "Control Lyapunov functions and hybrid zero dynamics," in 2012 IEEE 51st Conference on Decision and Control (CDC), 2012, pp. 6837–6842.
- [9] Q. Nguyen and K. Sreenath, "Exponential control barrier functions for enforcing high relative-degree safety-critical constraints," in 2016 American Control Conference (ACC), 2016, pp. 322–328.
- [10] W. Xiao and C. Belta, "High-order control barrier functions," *IEEE Transactions on Automatic Control*, vol. 67, no. 7, pp. 3655–3662, 2021
- [11] A. Isaly, B. C. Allen, R. G. Sanfelice, and W. E. Dixon, "Zeroing control barrier functions for safe volitional pedaling in a motorized cycle," *IFAC-PapersOnLine*, vol. 53, no. 5, pp. 218–223, 2020.
- [12] S. Liu, W. Xiao, and C. A. Belta, "Auxiliary-variable adaptive control barrier functions for safety critical systems," in 2023 62th IEEE Conference on Decision and Control (CDC), 2023.
- [13] —, "Auxiliary-variable adaptive control barrier functions," arXiv preprint arXiv:2502.15026, 2025.
- [14] C. Khazoom, D. Gonzalez-Diaz, Y. Ding, and S. Kim, "Humanoid self-collision avoidance using whole-body control with control barrier functions," in 2022 IEEE-RAS 21st International Conference on Humanoid Robots (Humanoids), 2022, pp. 558–565.
- [15] S. Liu, Z. Huang, J. Zeng, K. Sreenath, and C. A. Belta, "Learning-enabled iterative convex optimization for safety-critical model predictive control," *IEEE Open Journal of Control Systems*, 2025.
- [16] S. Liu, Y. Mao, and C. A. Belta, "Safety-critical planning and control for dynamic obstacle avoidance using control barrier functions," in 2025 American Control Conference (ACC), 2025, pp. 348–354.
- [17] L. Lindemann and D. V. Dimarogonas, "Control barrier functions for signal temporal logic tasks," *IEEE control systems letters*, vol. 3, no. 1, pp. 96–101, 2018.
- [18] W. Xiao, C. A. Belta, and C. G. Cassandras, "High order control Lyapunov-barrier functions for temporal logic specifications," in 2021 American Control Conference (ACC), 2021, pp. 4886–4891.
- [19] K. Garg and D. Panagou, "Control-lyapunov and control-barrier functions based quadratic program for spatio-temporal specifications," in 2019 IEEE 58th Conference on Decision and Control (CDC). IEEE, 2019, pp. 1422–1429.
- [20] S. Liu, W. Xiao, and C. A. Belta, "Auxiliary-variable adaptive control lyapunov barrier functions for spatio-temporally constrained safetycritical applications," in 2024 IEEE 63rd Conference on Decision and Control (CDC), 2024, pp. 8098–8104.
- [21] S.-C. Hsu, X. Xu, and A. D. Ames, "Control barrier function based quadratic programs with application to bipedal robotic walking," in 2015 American Control Conference (ACC), 2015, pp. 4542–4548.
- [22] G. Yang, C. Belta, and R. Tron, "Continuous-time signal temporal logic planning with control barrier functions," in 2020 American Control Conference (ACC), 2020, pp. 4612–4618.
- [23] W. S. Cortez, D. Oetomo, C. Manzie, and P. Choong, "Control barrier functions for mechanical systems: Theory and application to robotic grasping," *IEEE Transactions on Control Systems Technology*, vol. 29, no. 2, pp. 530–545, 2019.
- [24] G. Yang, C. Belta, and R. Tron, "Self-triggered control for safety critical systems using control barrier functions," in 2019 American control conference (ACC), 2019, pp. 4454–4459.
- [25] J. Breeden, K. Garg, and D. Panagou, "Control barrier functions in sampled-data systems," *IEEE Control Systems Letters*, vol. 6, pp. 367– 372, 2021.
- [26] A. J. Taylor, V. D. Dorobantu, R. K. Cosner, Y. Yue, and A. D. Ames, "Safety of sampled-data systems with control barrier functions via approximate discrete time models," in 2022 IEEE 61st Conference on Decision and Control (CDC), 2022, pp. 7127–7134.
- [27] L. Niu, B. Ramasubramanian, A. Clark, and R. Poovendran, "Sampling and quantization-aware control barrier functions for safety-critical control of cyber-physical systems," in 2024 IEEE 63rd Conference on Decision and Control (CDC), 2024, pp. 1637–1644.
- [28] R. T. Rockafellar and R. J. Wets, Variational analysis. Springer, 1998.
- [29] H. K. Khalil, Nonlinear systems; 3rd ed. Upper Saddle River, NJ: Prentice-Hall, 2002, the book can be consulted by contacting: PH-AID: Wallet, Lionel. [Online]. Available: https://cds.cern.ch/record/1173048
- [30] A. Singletary, Y. Chen, and A. D. Ames, "Control barrier functions for sampled-data systems with input delays," in 2020 59th IEEE Conference on Decision and Control (CDC), 2020, pp. 804–809.
- [31] W. Rudin, Principles of Mathematical Analysis, 3rd ed. McGraw-Hill, 1976
- [32] W. H. Press, S. A. Teukolsky, W. T. Vetterling, and B. P. Flannery, "Numerical recipes 3rd edition," *Cambridge: New York*, 2007.